

**Figure 2.** ORTEP view of **2** showing the atom-numbering scheme. Key bond lengths (Å) and angles (deg) not in text are as follows: Ru(1)–P(1) 2.378 (1), Ru(2)–P(1) 2.399 (1), Ru(2)–P(2) 2.401 (1), Ru(3)–P(2) 2.371 (1); Ru(1)–P(1)–Ru(2) 78.04 (3), Ru(2)–P(2)–Ru(3) 78.99 (3). A complete listing is provided in the Supplementary Material.<sup>9</sup>

I. Although the rupture of the Ru(1)–Ru(3) bond accompanied by the addition of H<sub>2</sub> might be expected to lead to a molecule in which the terminal hydrides point *toward* each other, the geometries of Ru(1) and Ru(3) indicate that the terminal hydrides are located at sites which are pointing *away* from each other on the back side of the molecule. Thus the terminal hydride on Ru(1) is positioned trans to C(3) and that on Ru(3) is trans to C(8). One simple explanation for this is that on addition of H<sub>2</sub> to the molecule, the  $\mu$ -H atoms already present in **1** swing back and occupy the terminal positions. The incoming H<sub>2</sub> molecule then provides an H atom in each of the new  $\mu$ -H locations. In solution there is exchange of terminal and bridging hydrides, and so we have been unable to verify this suggestion by D<sub>2</sub> labeling experiments.

The <sup>31</sup>P{<sup>1</sup>H} NMR spectrum for **2** is a singlet at +25 °C, while the <sup>1</sup>H NMR shows a second-order multiplet for the *t*-Bu<sub>2</sub>P protons. This signal consists of two sets of sharp outer lines ( $\delta$  1.50, 1.48 and  $\delta$  1.45, 1.44) which appear on either side of a broad inner peak at  $\delta$  1.47. At +40 °C all the peaks sharpen, and six lines can be observed at  $\delta$  1.66, 1.64, 1.63, 1.61, 1.60, and 1.59. At +25 °C, no signal to high field is observed. On cooling to –40 °C, two doublets are observed at  $\delta$  –9.36 (<sup>2</sup>*J*<sub>P-H</sub> = 18.0 Hz) and  $\delta$  –9.62 (<sup>2</sup>*J*<sub>P-H</sub> = 27.0 Hz), in addition to a broad singlet at  $\delta$  –17.08 (relative areas 1:1:2). The resonances to high field are assigned to the terminal and bridging hydrides, respectively. The *t*-Bu<sub>2</sub>P protons now appear as a very broad triplet ( $\delta$  1.44, apparent *J*<sub>P-H</sub> = 10.0 Hz). Although the solid-state structure indicates chemically equivalent terminal hydrides, the low-temperature spectrum suggests that in solution they are slightly nonequivalent. On warming to –20 °C, the two doublets at  $\delta$  –9.36 and  $\delta$  –9.62 broaden into two broad peaks ( $\delta$  –9.42,  $\delta$  –9.64), and the singlet at  $\delta$  –17.08 also broadens. Two broad resonances are observed at 0 °C ( $\delta$  –9.67 and  $\delta$  –17.08). At +60 °C, a single broad peak is observed at  $\delta$  –13.30, and this splits into two broad peaks at +80 °C ( $\delta$  –12.95,  $\delta$  –13.63). Clearly, the hydrides are fluxional at elevated temperatures, and the rapid exchange process is frozen out at low temperature. The *T*<sub>1</sub> values for all of these high field signals, both at +60 °C and –40 °C, are ca. 250 ms indicating that they are due to conventional hydride ligands and ruling out the possibility of molecular hydrogen ( $\eta^2$ -H<sub>2</sub>) species being present as dominant species.<sup>8</sup>

**Acknowledgment.** We thank the Robert A. Welch Foundation (F-816) and the National Science Foundation (CHE-8517759) for support. R.A.J. thanks the Alfred P. Sloan Foundation for a fellowship (1985–1989).

**Supplementary Material Available:** Experimental details of the synthesis and X-ray crystallography of **1** and **2** and tables of bond lengths, angles, positional parameters, and thermal parameters (17 pages); tables of observed and calculated structure factors (40 pages). Ordering information is given on any current masthead page.

(8) See, for example: Kubas, G. J. *Acc. Chem. Res.* **1988**, *21*, 120. Kubas, G. J.; Ryan, R. R.; Swanson, B. I.; Vergamini, P. J.; Wasserman, J. J. *J. Am. Chem. Soc.* **1984**, *106*, 451. Wasserman, J. J.; Kubas, G. J.; Ryan, R. R. *J. Am. Chem. Soc.* **1986**, *108*, 2294. Crabtree, R. H.; Lavin, M.; Bennevoit, L. *J. Am. Chem. Soc.* **1986**, *108*, 4032 and references therein.

(9) See paragraph at the end of the paper regarding Supplementary Material.

(10) **Note Added in Proof:** For a recent example of the reversible addition of H<sub>2</sub> to a Ru<sub>3</sub> phosphido cluster giving a phosphine (R<sub>2</sub>PH) unit, see: Lukan, N.; Lavigne, G.; Bonnet, J.-J.; Réau, R.; Neibecker, D.; Trachtenko, I. *J. Am. Chem. Soc.* **1988**, *110*, 5369.

## Biosynthesis of Marine Lipids. 19.<sup>1</sup> Dealkylation of the Sterol Side Chain in Sponges

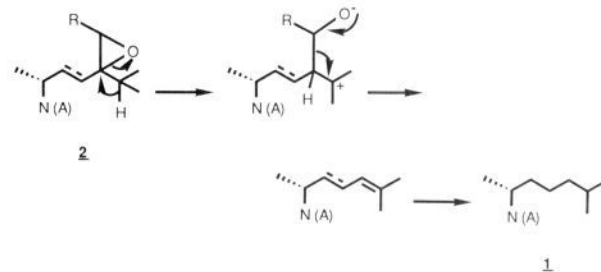
Sohail Malik, Russell G. Kerr, and Carl Djerassi\*

Department of Chemistry, Stanford University  
Stanford, California 94305

Received April 11, 1988

Recently, we have shown<sup>2</sup> unequivocally that some, but not all, sponges are capable of de novo synthesis of unusual as well as conventional sterols. We now report the first documentation that cholesterol (**1**) can be produced in sponges by dealkylation of 24(28)-unsaturated precursors, that the reaction proceeds through the same epoxide intermediate **2** operative in insects,<sup>3</sup> and most strikingly, that this dealkylation can occur in sponges that are capable of de novo sterol biosynthesis and side-chain alkylation. Therefore, Goad's comment<sup>4</sup> that "it would certainly be an extraordinary situation if animals of the same phylum have evolved the enzyme systems required for both C-24 alkylation and C-24 dealkylation reactions" seems to apply to a real situation.

Sterols, notably cholesterol (**1**), are required by insects, even though arthropods are incapable of de novo sterol biosynthesis. Clark and Bloch,<sup>5</sup> and later many other investigators,<sup>6</sup> have shown that insects are capable of dealkylating C-24 substituted plant sterols obtained from the diet by a mechanism that has been summarized by Ikekawa<sup>3a</sup> and Svoboda.<sup>3b</sup> Its key feature is the intermediacy of a 24,28-epoxide (**2**).



(1) For part 18, see: Malik, S.; Stoilov, I. L.; Djerassi, C. *Tetrahedron Lett.*, in press.

(2) Kerr, R. G.; Stoilov, I. L.; Thompson, J. E.; Djerassi, C. *Tetrahedron*, submitted for publication.

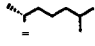
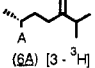
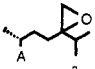
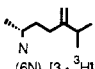
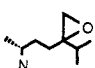
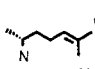
(3) (a) Ikekawa, N. In *Sterols and Bile Acids*; Danielsson, H., Sjövall, J., Eds.; Elsevier: Amsterdam, 1985; pp 199–230. (b) Svoboda, J. A. In *Isopentenoids in Plants*; Nes, W. D., Fuller, G., Tsai, L., Eds.; Marcel Dekker: New York, 1984; pp 367–388.

(4) Goad, L. J. *Pure Appl. Chem.* **1981**, *51*, 837–852.

(5) Clark, A. J.; Bloch, K. *J. Biol. Chem.* **1959**, *234*, 2589–2594.

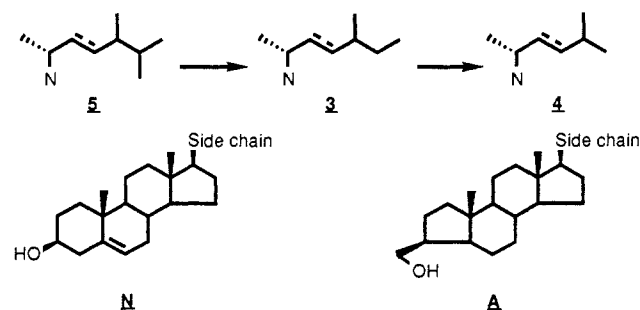
(6) For leading references, see: Thompson, M. J.; Kaplanis, J. N.; Robbins, W. E.; Svoboda, J. A. *Adv. Lipid Res.* **1973**, *11*, 219–265.

**Table I.** Incorporation of Sterol Precursors into Cholesterol (1) in Four Sponges

precursor <sup>a</sup>	radioactivity fed, dpm (recovered radioactivity in precursor)  (recovered radioactivity in total sterol mixture)	sponge	Radioactivity recovered in  (mg) <sup>b</sup> , (dpm) <sup>c</sup> , (dpm/mg) <sup>d</sup> , (%) <sup>e</sup>
 (6A) [3- <sup>3</sup> H]	9.24 × 10 <sup>7</sup> (1 067 866) (4 319 895)	<i>Phakellia aruensis</i>	(33), (450 101), (85 246), (10.4)
"	2.2 × 10 <sup>7</sup> (148 151) (506 310)	<i>Axinella verrucosa</i>	(30), (20 646), (1721), (4.1)
 (2A) [3- <sup>3</sup> H]	2.2 × 10 <sup>7</sup> (405 860) (812 732)	<i>Phakellia aruensis</i>	(56), (257 541), (28 743), (31.7)
"	1.54 × 10 <sup>7</sup> (46 680) (94 992)	<i>Axinella verrucosa</i>	(15), (14 154), (2359), (14.9)
 (6N) [3- <sup>3</sup> H]	4.4 × 10 <sup>7</sup> (288 603) (482 979)	<i>Tethya aurantia californiana</i>	(34), (31 064), (1849), (6.4)
"	4.4 × 10 <sup>7</sup> (454 572) (1 025 703)	<i>Microciona prolifera</i>	(23), (184 562), (13 897), (17.9)
 (2N) [3- <sup>3</sup> H]	4.4 × 10 <sup>7</sup> (cold) (1 025 244)	<i>Tethya aurantia californiana</i>	(40), (861 624), (50 683), (84.0)
"	4.4 × 10 <sup>7</sup> (4 500) (1 425 506)	<i>Microciona prolifera</i>	(25), (616 438), (34 247), (43.2)
 (7N) [24- <sup>14</sup> C]	1.1 × 10 <sup>7</sup> (120 420) (2 010 474)	<i>Tethya aurantia californiana</i>	(39), (893 025), (54 123), (44.4)

<sup>a</sup>The radiolabeled precursors were synthesized from the naturally occurring sterols by previously described<sup>1,16</sup> methods. The radiolabeled epoxides were made by treating 6A and 6N with *m*-CPBA under standard conditions. (Purity of precursors and products is based upon HPLC and capillary GC analysis.) <sup>b</sup>Weight of total sterol mixture. <sup>c</sup>Total radioactivity. <sup>d</sup>Specific radioactivity. <sup>e</sup>Percent recovered radioactivity with respect to the total sterol mixture. <sup>f</sup>When desmosterol (7N) was used as a precursor, (917 136 dpm), (152 856 dpm/mg) (45.6%), radioactivity was recovered in 24-methylenecholesterol (6N). (All experiments were performed in duplicate.)

In the 1970s, it was noted that certain gastropod molluscs,<sup>7</sup> crustaceans,<sup>8</sup> and coelenterates<sup>9</sup> are also capable of such dealkylations, although the precise mechanism has not been established for these marine organisms. Until now, no one has demonstrated such dealkylation in sponges; however, it has been hypothesized<sup>10</sup> that two unique types of marine sterols—the C<sub>27</sub> norergostanes (3)<sup>11</sup> and the C<sub>26</sub> 24-nor sterols (4)<sup>12</sup>—may formally arise by one



or two such dealkylations of the terminal carbons from 24-

methylated precursors (5). The question of sterol side-chain dealkylation in sponges, therefore, has potential implications beyond those of the generation of the cholesterol-type side-chain.

The phylum Porifera, occupying the bottom of the evolutionary scale of eucaryotes, is unusual in that, on the one hand, many sponges are sources of uniquely polyalkylated sterol side-chains,<sup>3a,10</sup> while some others contain,<sup>13</sup> partly or totally, conventional sterols of the cholesterol (1) or 24-alkyl (5) type.

As summarized in Table I, by feeding suitable radioactive precursors by a previously described<sup>14</sup> method, for ca. 1 month, we have demonstrated such dealkylations in *Phakellia aruensis* and *Axinella verrucosa*—two sponges that have been shown<sup>2,15</sup> to use dietary precursors for ring contraction to their unique A-nor sterol nuclei (A)—as well as in *Microciona prolifera* and *Tethya aurantia californiana*, which contain conventional sterols (N) synthesized<sup>2</sup> de novo via cycloartenol as well as lanosterol.

The efficient utilization of the 24,28-epoxides 2A and 2N (Table I) by sponges suggests that they are intermediates in the dealkylation process. This implies that the same mechanism (2 → 1) operating in insects<sup>3</sup> also occurs in sponges and presumably proceeds via a 24-dehydro intermediate (7). While neither the epoxides (2A or 2N) nor the appropriate desmosterols (7A or 7N) have been detected in these four sponges, an experiment conducted in *T. aurantia* demonstrates (Table I) that labeled desmosterol (7N) is efficiently transformed into cholesterol (1) as well as

(7) Collignon-Thiennot, F.; Allais, J. P.; Barbier, M. *Biochimie* **1973**, *55*, 579–582. Khalil, M. W.; Idler, D. R. *Comp. Biochem. Physiol.* **1976**, *55B*, 239–242. Teshima, S.; Kanazawa, A.; Miyawaki, H. *Comp. Biochem. Physiol.* **1979**, *63B*, 323–328.

(8) Teshima, S.; Kanazawa, A. *Comp. Biochem. Physiol.* **1971**, *38B*, 603–607. Kanazawa, A.; Guary, J. B.; Ceccaldi, H. *J. Comp. Biochem. Physiol.* **1976**, *54B*, 205–208.

(9) Salot, A.; Barbier, M. *J. Exp. Mar. Biol. Ecol.* **1973**, *13*, 207–214. (10) For leading references, see: Djerassi, C.; Theobald, N.; Kokke, W. C. M. C.; Pak, C. S.; Carlson, R. M. K. *Pure Appl. Chem.* **1979**, *51*, 1815–1828.

(11) For first isolation, see: Kobayashi, M.; Mitsuhashi, H. *Steroids* **1974**, *24*, 399–410.

(12) For first isolation, see: Idler, D. R.; Wiseman, P. M.; Safe, L. M. *Steroids* **1970**, *16*, 451–461.

(13) Goad, L. J. In *Biochemical and Biophysical Perspectives in Marine Biology*; Malins, D. C., Sargent, J. R., Eds.; Academic Press: New York, 1976; Vol. 3, pp 213–318.

(14) Catalan, C. A. N.; Thompson, J. E.; Kokke, W. C. M. C.; Djerassi, C. *Tetrahedron* **1985**, *41*, 1073–1084.

(15) De Rosa, M.; Minale, L.; Sodano, G. *Experientia* **1975**, *31*, 408–410. De Rosa, M.; Minale, L.; Sodano, G. *Experientia* **1976**, *32*, 1112–1113.

(16) Dayal, B.; Salen, G.; Tint, G. S.; Biswas, C. *Steroids* **1983**, *42*, 635–640.

24-methylenecholesterol (6N). In other words, this sponge is capable of de novo biosynthesis,<sup>2</sup> side-chain dealkylation (at C-24), and C-24 side-chain alkylation.

Experiments are under way to examine more precisely the course and scope of these dealkylations among sponge sterols.

**Acknowledgment.** We thank the National Institutes of Health (Grant no. GM-06840) for financial assistance and Jane Fromont and Christopher J. Silva for certain of the sponge incorporations.

### Internal Electron Transfer in a Quinone Adduct of a Nickel(II)-Catecholate Complex

Cristiano Benelli, Andrea Dei,\* Dante Gatteschi,\* and Luca Pardi

Department of Chemistry, University of Florence  
Florence, Italy

Received May 2, 1988

Quinoid molecules are known to form charge-transfer complexes where they behave either as donors or acceptors toward many organic molecules and to easily undergo redox processes.<sup>1</sup> In addition, they act as good ligands toward transition-metal ions.<sup>2,3</sup> Since the  $\pi$  electron levels of these molecules have energies comparable to 3d metal orbitals, transition-metal-quinoid adducts provide simulating perspectives for designing redox reagents characterized by peculiar reactivity properties. Recent studies aim at the elucidation of the role of quinoid molecules in naturally occurring reaction processes as well as in the synthesis of electron-transfer catalysts.<sup>4-9</sup>

Redox processes involving quinoid molecules and substrates often occur via formation of charge-transfer adducts, followed by electron transfer between the reactants. One may expect that a similar mechanism is operative when the quinoid molecule is coordinated to a metal ion, even if in this case the electron transfer may involve an electronic rearrangement within the metal quinoid adduct. Evidence exists that this mechanism is often operative, but an alternative reaction pathway must be considered, as the following results clearly show.

The Ni(TCCat) complex (L = 2,4,4-trimethyl-1,5,9-triaza-cyclododec-1-ene; TCCat = tetrachlorocatecholate) was synthesized from the reaction between the five-coordinate  $[\text{NiL}(\text{O}-\text{H})_2(\text{ClO}_4)_2]^{10}$  and tetrachlorocatechol. On the basis of the electronic spectra<sup>11</sup> and of magnetic measurements ( $\mu_{\text{eff}} = 3.22 \mu_{\text{B}}$ ) this compound may be formulated as a high spin five-coordinate nickel(II) catecholate adduct. We found that this compound reacts reversibly with tetrachloro-1,2-benzoquinone (TCQ) yielding a compound of formula "NiL(TCCat)(TCQ)". The reaction can be followed by the appearance in the electronic spectrum of an intense absorption band at  $12700 \text{ cm}^{-1}$  ( $\epsilon = 2000$

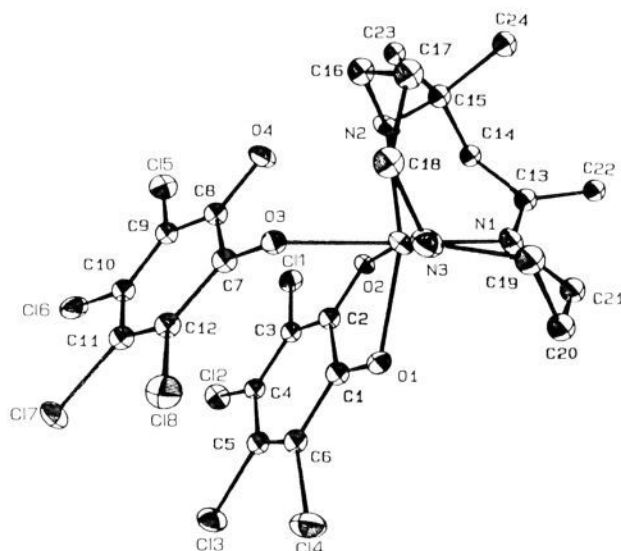


**Figure 1.** ORTEP view of the asymmetric unit of NiL(TCSQ)TCQ. Selected bond distances (pm) and angles (deg). Distances: Ni-O1 = 212 (1), Ni-O2 = 210 (1), Ni-O3 = 221 (1), Ni-N1 = 206 (2), Ni-N2 = 211 (1), Ni-N3 = 208 (2), C1-O1 = 125 (1), C2-O2 = 128 (1), C7-O3 = 123 (1), C8-O4 = 123 (1), C1-C2 = 147 (2), C2-C3 = 143 (2), C3-C4 = 142 (2), C4-C5 = 140 (2), C5-C6 = 134 (2), C1-C6 = 147 (2), C7-C8 = 151 (2), C8-C9, 142 (2); C9-C10, 139 (2), C10-C11 = 144 (2), C11-C12 = 131 (2). Angles: O1-Ni-O2 = 78.6 (0.4), O1-Ni-O3 = 79.1 (0.3), O1-Ni-N1 = 102.1 (0.4), O1-Ni-N2 = 162.3 (0.4), O2-Ni-O3 = 87.5 (0.3), O2-Ni-N1 = 95.7 (0.4), O2-Ni-N2 = 91.7 (0.4), O2-Ni-N3 = 164.6 (0.3), O3-Ni-N1 = 176.7 (0.4), O3-Ni-N2 = 85.7 (0.4), O3-Ni-N3 = 82.7 (0.4), N2-Ni-N1 = 93.6 (0.4), N1-Ni-N3 = 94.3 (0.5), N2-Ni-N3 = 99.3 (0.4).

$1 \text{ cm}^{-1} \text{ mol}^{-1}$ ). "NiL(TCCat)(TCQ)" can be isolated as a solid owing to its insolubility.

The X-ray crystal structure<sup>12</sup> of the adduct indicates that both dioxolene ligands are coordinated to the nickel ion in a highly distorted pseudooctahedral coordination geometry (Figure 1). One of the dioxolene ligands acts as bidentate and the other as monodentate. The Ni-O distances are significantly different for the two molecules, being 210 pm for the chelate and 221 pm for the monodentate ligands, respectively. The three nitrogen donors of the cyclic ligand occupy the remaining facial coordination sites.

The structural parameters of the coordinated dioxolene molecule have been taken as the main evidence for determining the nature of the ligand, i.e., quinone, semiquinone, or catecholate.<sup>2</sup> In the present case the structural parameters of the chelate dioxolene are consistent with the anionic semiquinone nature of this moiety, as shown by the average values of the C-O (127 pm) and of the C(1)-C(2) distances (147 pm). The structural parameters of the monodentate dioxolene on the other hand are close to those expected for the quinone form of the molecule, the C-O distances being 123 pm longer than those observed in the free molecule (120.8 pm),<sup>13</sup> but are significantly shorter than those expected for a reduced form of the dioxolene ligand. Moreover the other C-C distances within the ring are very close to those observed in the free quinone.

(12) Crystal and experimental data for the title compound:  $\text{C}_{24}\text{H}_{28}\text{N}_3\text{O}_4\text{Cl}_4\text{Ni}$ , monoclinic,  $P2_1/c$ ,  $a = 1450.2$  (5),  $b = 874.1$  (2),  $c = 2316.4$  (8),  $\beta = 98.92$  (3),  $V = 2.9008$  (1)  $\times 10^6 \text{ pm}^3$ ,  $Z = 4$ ,  $D_{\text{calc}} = 1.744 \text{ g cm}^{-3}$ ,  $\mu = 13.64 \text{ cm}^{-1}$ . A well-shaped crystal of dimension  $0.35 \times 0.30 \times 0.15$  was used for data collection (CAD4 Enraf Nonius diffractometer, Mo  $\text{K}\alpha$   $\lambda = 71.069 \text{ pm}$ , scan mode:  $\omega-2\theta$ , scan range:  $2.5 \leq \theta \leq 22.5$ , measured reflections:  $-15 \leq h \leq 15$ ,  $0 \leq k \leq 9$ ,  $0 \leq l \leq 25$ , total number 4200,  $F \geq 6\sigma(F)$  1938). Refinement of structure: Patterson map localized in Ni atom. The final refinement with hydrogen atoms in fixed idealized position converged with  $R = 0.060$ ,  $R_w = 0.056$ . Computer programs used in the structure solution are reported in the following: ShelDRICK, G. SHELX76 System of Computing Programs; University of Cambridge, England, 1976. Johnson, C. K. ORTEP, Report ORNL 3.794; Oak Ridge National Laboratory: Oak Ridge, TN, 1965.

(13) Zanotti, G.; Del Pra, A. *Acta Crystallogr.* **1978**, *B34*, 2997.

(1) *The Chemistry of Quinoid Compounds*; Patai, S. Ed.; Wiley: New York, 1974.

(2) Pierpont, C. G.; Buchanan, R. M. *Coord. Chem. Rev.* **1981**, *38*, 45.

(3) Kaim, W. *Coord. Chem. Rev.* **1987**, *76*, 187.

(4) Buchanan, R. M.; Pierpont, C. G. *J. Am. Chem. Soc.* **1980**, *102*, 4951.

(5) Lynch, M. W.; Valentine, M.; Hendrickson, D. N. *J. Am. Chem. Soc.* **1982**, *104*, 6982.

(6) Lynch, M. W.; Hendrickson, D. N.; Fitzgerald, B. J.; Pierpont, C. G. *J. Am. Chem. Soc.* **1984**, *106*, 2041.

(7) Cass, M. E.; Gordon, N. R.; Pierpont, C. G. *Inorg. Chem.* **1986**, *25*, 3962.

(8) Haga, M.; Dodsworth, E. S.; Lever, A. B. P. *Inorg. Chem.* **1986**, *25*, 447.

(9) Thompson, J. S.; Calabrese, J. C. *Inorg. Chem.* **1985**, *24*, 3167.

(10) Martin, J. W. L.; Johnston, J. H.; Curtis, N. F. *J. Chem. Soc., Dalton Trans.* **1978**, 68.

(11) Its electronic spectrum shows bands at  $7000$  ( $\epsilon = 55 \text{ l cm}^{-1} \text{ mol}^{-1}$ ),  $12500$  ( $\epsilon = 20 \text{ l cm}^{-1} \text{ mol}^{-1}$ ), and  $17400$  ( $\epsilon = 60 \text{ l cm}^{-1} \text{ mol}^{-1}$ )  $\text{cm}^{-1}$ , respectively, supporting the formulation of five-coordinate nickel(II)-catecholate adduct. More intense bands occurring at  $23400$  ( $\epsilon = 1800 \text{ l cm}^{-1} \text{ mol}^{-1}$ ) and  $25700$  ( $\epsilon = 1900 \text{ l cm}^{-1} \text{ mol}^{-1}$ ) are assigned to LMCT transitions.